

Validation of SIMIND Monte Carlo for ^{99m}Tc and ^{177}Lu

Giovanni Di Domenico (✉ ddmgnn@unife.it)

University of Ferrara Department of Physics: Università degli Studi di Ferrara Dipartimento di Fisica e Scienze della Terra <https://orcid.org/0000-0002-8500-6764>

Simona Di Biaso

University of Ferrara Department of Physics: Università degli Studi di Ferrara Dipartimento di Fisica e Scienze della Terra

Lorenzo Longo

University of Ferrara Department of Physics: Università degli Studi di Ferrara Dipartimento di Fisica e Scienze della Terra

Alessandro Turra

Medical Physics Unit, University Hospital, Ferrara

Eugenia Tonini

Medical Physics Unit; University Hospital, Ferrara

Maria Concetta Longo

San Bortolo Hospital: Ospedale San Bortolo di Vicenza

Licia Uccelli

University of Ferrara Department of Translational Medicine

Mirco Bartolomei

Nuclear Medicine Unit, University Hospital, Ferrara

Original research

Keywords: quantitative imaging, molecular radiotherapy, SIMIND Monte Carlo code, quantitative activity estimation

Posted Date: July 1st, 2022

DOI: <https://doi.org/10.21203/rs.3.rs-1756734/v1>

License:   This work is licensed under a Creative Commons Attribution 4.0 International License.

[Read Full License](#)

RESEARCH

Validation of SIMIND Monte Carlo for ^{99m}Tc and ^{177}Lu

Giovanni Di Domenico^{1*}, Simona Di Biaso¹, Lorenzo Longo¹, Alessandro Turra², Eugenia Tonini², MariaConcetta Longo³, Licia Uccelli^{4,5} and Mirco Bartolomei⁴

*Correspondence: ddmgnn@unife.it

¹Department of Physics and Earth Science, University of Ferrara, via Saragat 1, 44122 Ferrara, IT

Full list of author information is available at the end of the article

Abstract

Purpose: Monte Carlo (MC) simulation in Nuclear Medicine is a powerful tool for modelling many physical phenomena which are difficult to track or to measure directly. MC simulation in SPECT/CT imaging is particularly suitable for optimizing the quantification of activity in a patient, and, consequently, the absorbed dose to each organ. To do so, it is mandatory validate MC results with real data acquired with gamma camera. The aim of this study was the validation of SIMIND Monte Carlo code for modelling a Siemens Symbia Intevo Excel SPECT-CT gamma camera both for ^{99m}Tc and ^{177}Lu .

Methods: Phantom experiments using ^{99m}Tc and ^{177}Lu have been performed with the purpose to measure spatial resolution, sensitivity and evaluate the calibration factor (CF) and recovery coefficients (RC) from acquired data. The geometries used for 2D planar imaging were (1) Petri dish and (2) capillary source while for 3D volumetric imaging were (3) a uniform filled cylinder phantom and (4) a Jaszczack phantom with spheres with different volumes. The experimental results have been compared with the results obtained from Monte Carlo simulations performed in the same geometries.

Results: Comparison shows good accordance between simulated and experimental data. The measured planar spatial resolution was 8.3 ± 0.8 mm for ^{99m}Tc and 12.2 ± 0.7 mm for ^{177}Lu . The corresponding data obtained by SIMIND for ^{99m}Tc was 7.4 ± 0.1 mm, while for ^{177}Lu was 11.7 ± 0.1 mm. The CF was 110.1 ± 5.5 cps/MBq for Technetium and 18.3 ± 1.0 cps/MBq for Lutetium. The corresponding CF obtained by SIMIND for ^{99m}Tc was 100.1 ± 0.3 cps/MBq, while for ^{177}Lu 20.4 ± 0.7 cps/MBq. Moreover, a complete curve RCs vs Volume (ml) both for Technetium and Lutetium was determined to correct the PVE for all volumes of clinical interest. In none of the cases a RC factor equal to 100 was found.

Conclusions: The results of validation process show that SIMIND can be used for simulating both gamma camera planar and SPECT images of Siemens Symbia Intevo using ^{99m}Tc and ^{177}Lu radionuclides for different medical purposes and treatments.

Keywords: quantitative imaging; molecular radiotherapy; SIMIND Monte Carlo code; quantitative activity estimation

Background

In modern nuclear medicine, the absolute quantification of SPECT images is fundamental for providing an estimate of the activity uptake in various organs and tissues for the purpose of diagnostic assessments and therapeutic decisions. Monte

1
2
3
4
5 Carlo (MC) simulation is a tool widely used to model real life systems, including
6 nuclear medicine devices [1]. Starting from the description of particles interaction
7 with matter, by using probability density functions (pdfs) and with the help of ran-
8 dom number generators and sampling techniques, MC provides the opportunity to
9 analyze the phenomena of physics underlying the formation of images with the aim
10 of optimizing the data acquisition and processing steps. Due to the approximation
11 and the simplification used in the description of physics laws inside a MC code, a
12 mandatory step is the validation of MC model (code) before using it to simulate
13 real world systems, in particular as a clinical simulator for SPECT imaging. To
14 validate a MC code, outputs of simulated experiments are compared against results
15 obtained from experimental measurements on the physical system. The validation
16 ensures that the simulated system truly is in fact the physical one.

17
18
19
20
21 The absolute activity quantification consists in several steps: the first one is to
22 reconstruct projection images, taking into account photon attenuation, scatter and
23 Collimator Detector Response (CDR). CDR is one of the most degrading factors in
24 SPECT imaging [2]. It is caused by several factors: photons which pass through the
25 holes' septa and photons which, despite the scattering with hole septa, have been
26 detected. For modeling the scanner CDR one can use a capillary source placed at
27 several source-to-detector distances while keeping the rotation angle fixed [3]. Us-
28 ually, the Gaussian + exponential function fits the measurements, and the fit results
29 are used to model the distance-dependent CDR. The second step is to convert the
30 reconstructed counts per second into activity [in MBq] through a Calibration Factor
31 (CF). Different camera calibration methods have been proposed for evaluating CF:
32 some researchers use planar scans of a small source [4] or of a petri dish (following
33 NEMA protocol for camera sensitivity test) [5], other ones use tomographic scans
34 of a very simple phantom, such as a large cylindrical phantom (to avoid Partial Vol-
35 ume Effect, PVE), with a certain, known activity inside[6]. The CF unit is cps/MBq
36 and it should be computed for every radionuclide and collimator used. The last step
37 is to compute recovery coefficient (RC) factors in order to correct for the PVE: for
38 small volumes, measured activity appears to be distributed among a larger volume
39 respect to the actual one; this may lead to an underestimation of the activity in
40 the real volume (and, then, of the measured absorbed dose) and to a wrong volume
41 estimation. This is due to blurring effect, caused by a finite spatial resolution. PVE
42 can be estimated through phantom studies, using Jaszczak phantom with known
43 volume spheres. The RC factors are equal to the ratio between the measured activ-
44 ity in each sphere and the true one and it is expressed in percentage; they will be
45 used to correct the final activity inside each sphere.

46
47
48
49
50
51
52 Some authors have reported the comparison of measured and simulated gamma
53 camera performances like spatial resolution, planar sensitivity, CF and RC for
54 ^{99m}Tc , ^{177}Lu or radionuclides with photons of energy higher than 140 keV
55 [7, 8, 9, 10], both to investigate the influence a parameter has on systems' per-
56 formances and to validate the MC codes' capability in modelling a specific gamma
57 camera to use it later as a clinical simulator [11].

58
59
60
61
62
63
64
65
66
67
68
69
70
71
72
73
74
75
76
77
78
79
80
81
82
83
84
85
86
87
88
89
90
91
92
93
94
95
96
97
98
99
100
101
102
103
104
105
106
107
108
109
110
111
112
113
114
115
116
117
118
119
120
121
122
123
124
125
126
127
128
129
130
131
132
133
134
135
136
137
138
139
140
141
142
143
144
145
146
147
148
149
150
151
152
153
154
155
156
157
158
159
160
161
162
163
164
165
166
167
168
169
170
171
172
173
174
175
176
177
178
179
180
181
182
183
184
185
186
187
188
189
190
191
192
193
194
195
196
197
198
199
200
201
202
203
204
205
206
207
208
209
210
211
212
213
214
215
216
217
218
219
220
221
222
223
224
225
226
227
228
229
230
231
232
233
234
235
236
237
238
239
240
241
242
243
244
245
246
247
248
249
250
251
252
253
254
255
256
257
258
259
260
261
262
263
264
265
266
267
268
269
270
271
272
273
274
275
276
277
278
279
280
281
282
283
284
285
286
287
288
289
290
291
292
293
294
295
296
297
298
299
300
301
302
303
304
305
306
307
308
309
310
311
312
313
314
315
316
317
318
319
320
321
322
323
324
325
326
327
328
329
330
331
332
333
334
335
336
337
338
339
340
341
342
343
344
345
346
347
348
349
350
351
352
353
354
355
356
357
358
359
360
361
362
363
364
365
366
367
368
369
370
371
372
373
374
375
376
377
378
379
380
381
382
383
384
385
386
387
388
389
390
391
392
393
394
395
396
397
398
399
400
401
402
403
404
405
406
407
408
409
410
411
412
413
414
415
416
417
418
419
420
421
422
423
424
425
426
427
428
429
430
431
432
433
434
435
436
437
438
439
440
441
442
443
444
445
446
447
448
449
450
451
452
453
454
455
456
457
458
459
460
461
462
463
464
465
466
467
468
469
470
471
472
473
474
475
476
477
478
479
480
481
482
483
484
485
486
487
488
489
490
491
492
493
494
495
496
497
498
499
500
501
502
503
504
505
506
507
508
509
510
511
512
513
514
515
516
517
518
519
520
521
522
523
524
525
526
527
528
529
530
531
532
533
534
535
536
537
538
539
540
541
542
543
544
545
546
547
548
549
550
551
552
553
554
555
556
557
558
559
560
561
562
563
564
565
566
567
568
569
570
571
572
573
574
575
576
577
578
579
580
581
582
583
584
585
586
587
588
589
590
591
592
593
594
595
596
597
598
599
600
601
602
603
604
605
606
607
608
609
610
611
612
613
614
615
616
617
618
619
620
621
622
623
624
625
626
627
628
629
630
631
632
633
634
635
636
637
638
639
640
641
642
643
644
645
646
647
648
649
650
651
652
653
654
655
656
657
658
659
660
661
662
663
664
665
666
667
668
669
670
671
672
673
674
675
676
677
678
679
680
681
682
683
684
685
686
687
688
689
690
691
692
693
694
695
696
697
698
699
700
701
702
703
704
705
706
707
708
709
710
711
712
713
714
715
716
717
718
719
720
721
722
723
724
725
726
727
728
729
730
731
732
733
734
735
736
737
738
739
740
741
742
743
744
745
746
747
748
749
750
751
752
753
754
755
756
757
758
759
760
761
762
763
764
765
766
767
768
769
770
771
772
773
774
775
776
777
778
779
780
781
782
783
784
785
786
787
788
789
790
791
792
793
794
795
796
797
798
799
800
801
802
803
804
805
806
807
808
809
810
811
812
813
814
815
816
817
818
819
820
821
822
823
824
825
826
827
828
829
830
831
832
833
834
835
836
837
838
839
840
841
842
843
844
845
846
847
848
849
850
851
852
853
854
855
856
857
858
859
860
861
862
863
864
865
866
867
868
869
870
871
872
873
874
875
876
877
878
879
880
881
882
883
884
885
886
887
888
889
890
891
892
893
894
895
896
897
898
899
900
901
902
903
904
905
906
907
908
909
910
911
912
913
914
915
916
917
918
919
920
921
922
923
924
925
926
927
928
929
930
931
932
933
934
935
936
937
938
939
940
941
942
943
944
945
946
947
948
949
950
951
952
953
954
955
956
957
958
959
960
961
962
963
964
965
966
967
968
969
970
971
972
973
974
975
976
977
978
979
980
981
982
983
984
985
986
987
988
989
990
991
992
993
994
995
996
997
998
999
1000

simulation. To this aim, a Siemens Symbia Intevo Excel SPECT/CT scintillation camera has been modelled by using the SIMIND Monte Carlo Program (version 6.1) [12]. Planar and tomographic studies have been performed for two radioisotopes: ^{99m}Tc the most used radionuclide in SPECT/CT imaging studies, and ^{177}Lu an attractive radionuclide used for peptide receptor radionuclide therapy (PRRT) using the theranostic approach [13]. Moreover, RC factors have been evaluated both for ^{99m}Tc and ^{177}Lu .

Materials and methods

This study is composed of two parts: experimental data acquisition and Monte Carlo simulations. In each part both ^{99m}Tc and ^{177}Lu radioisotopes are studied, for a total of 40 experimental scans and 140 simulation runs. The information about the isotopes' half-lives, their main gamma emissions and the maximum energy of their beta emission are summarized in Table 1.

The SPECT/CT scanner used for the experimental measurements is a Siemens Symbia Intevo Excel provided by Nuclear Medicine Unit, University Hospital of Ferrara (Italy). The system is equipped by two gamma camera heads with NaI scintillator crystals (FOV 53.3x38.7 cm). The gamma camera parameters are listed in Table 2. The so-called "step and shot" technique was used for the tomographic studies. The CT was performed after the SPECT acquisition, with a 110 kV voltage and Care Dose 4D. The Symbia Intevo Excel was equipped with a Low Energy High Resolution (SY-LEHR) collimator for ^{99m}Tc studies and with a Medium Energy Low Purpose collimator (SY-MELP) for ^{177}Lu studies. A Mec Murphil MP-DC-Chamber dose calibrator has been used for the activity measurement. Activities have been assessed by performing five measurements of the syringes containing the isotopes, subtracting the residual activity. The ^{99m}Tc radioisotope has been obtained as sodium pertechnetate ($\text{Na}[^{99m}\text{Tc}]\text{O}_4$) from $^{99}\text{Mo}/^{99m}\text{Tc}$ generator (Ultratechnekow, CURIMUM, Netherlands), while the ^{177}Lu has been obtained as Lutetium chloride ($[^{177}\text{Lu}]\text{Cl}_3$) (EndoLucinBeta, ITM, Munich, Germany).

Phantom experiments for ^{99m}Tc and ^{177}Lu : planar imaging

Planar measurements aim at the evaluation of the fundamental SPECT features: spatial resolution and sensitivity, which are defined by the scintillation crystal and the collimator. In order to characterize the main properties of the Symbia Intevo gamma camera's, one at a time the two heads have been exploited.

The gamma camera data were acquired with a 15% energy window centered on the 140.5 keV for the main photopeak of the ^{99m}Tc , and with two 15% energy windows centered on the 113 keV and 208 keV photopeaks of the ^{177}Lu . All measurements have been repeated three times and performed with different distances between the source and the detector.

Extrinsic spatial resolution measurement

A capillary tube with an inner diameter of 1 mm was used to determine the system spatial resolution. The tube was filled with 30 ± 1 MBq of a ^{99m}Tc solution and with a 130 ± 7 MBq of a ^{177}Lu solution.

In order to study the spatial resolution, the tube was placed at three different distances from the front face of collimator for the experimental measurements: 10.0 ± 0.5 cm, 25.0 ± 0.5 cm and 35 ± 0.5 cm.

The spatial resolution was measured by drawing a profile across the image of the capillary tube in three different positions in order to compensate for the possible non-uniformity in the tube filling. The line profile was fitted with a Gaussian function from whose full width at half maximum (FWHM) and the full width at tenth maximum (FWTM) were calculated. The reference value provided by SIEMENS for the extrinsic spatial resolution with a LEHR collimator and a capillary tube filled with a ^{99m}Tc source is 7.5 mm at 10 cm.

System sensitivity measurement

A Petri Dish with an inner diameter of 10 cm was filled with 25.0 ± 1.3 MBq of a ^{99m}Tc solution and with a 30.0 ± 1.5 MBq of a ^{177}Lu solution. The reference value provided by SIEMENS for the sensitivity with a LEHR collimator and a Petri dish filled with a ^{99m}Tc source is 91.8 cps/MBq at 10 cm.

Phantom experiments for ^{99m}Tc and ^{177}Lu : tomographic imaging

Calibration Factor measurement

A cylindrical Jaszczak SPECT Phantom (figure 1) deprived of the inner spheres has been employed to obtain the CF. The cylinder was filled with a 6800 ml solution of distilled water, 350 MBq of ^{99m}Tc .

Similarly, the uniform Jaszczak phantom was filled with a 6800 ml solution of distilled water (6720 ml), 2810 MBq of ^{177}Lu from a certificated vial with an accuracy of $\pm 10\%$, 67ml of HCl (37%) added in order to make the solution the most homogeneous as possible and to avoid lutetium accumulation on phantom borders.

Both for ^{99m}Tc and ^{177}Lu , the SPECT/CT acquisitions were performed via the Siemens Symbia Intevo Excel with the step-and-shoot technique. Each tomographic acquisition consisted in 64 projections performed maintaining a constant distance of 25 cm between the center of the cylinder and the lower part of the detector head. The acquisition time was of 10 s or 20 s for ^{99m}Tc , while it was of 30 s for ^{177}Lu .

The reconstruction of the projected images was performed with the built-in software from the vendor, Siemens Flash3D. The OSEM 3D was the iteration reconstruction technique chosen, with 10 iterations and 8 subsets. The Flash3D is capable of applying attenuation, scatter and CDR corrections.

The scatter correction for Technetium was performed via the DEW (Double Energy Windows) technique with the use of the PW (Peak Window) and the LSW (Lower Scatter Window).

The scatter correction for Lutetium was performed via the TEW (Triple Energy Windows) method for the 113 keV peak and the DEW method for 208 keV peak; the widths of each photopeak window are reported in Table 3.

Recovery coefficients measurement

In order to obtain the RC factors, the absolute quantification of ^{99m}Tc was performed via a Jaszczak SPECT Phantom with six hot spheres.

The phantom was placed in the center of the field of view. Acquisitions were performed with the same settings as those of the uniformly filled Jaszczak phantom

previously described and conducted with 64 projections of 10 s or 20 s scan time. The energy windows are the same as those set for the CF evaluation and are listed in Table 3. The spheres volume and the background activity are listed in Table 4. Each activity value reported in Table 4 is the mean of five different measurements. For the evaluation of the RC factors of ^{177}Lu a NEMA image quality PET phantom with five spheres of different diameters was used. Spheres diameters, volumes, injected and background activities are listed in the Table 5. Measurement settings are the same as those used for the CF evaluation and are listed in Table 2 and Table 3. The number of projections was 64, each of 30 s duration.

The ratio between activity concentration in the background and the activity concentration in the spheres is 1:45. Each value reported in this Table 5 is the mean of five different measurements, with an associated standard deviation of less than 1%. The process of activity measurement is the same as that described for the ^{99m}Tc . CT data has been used for the delineation of volume of interest (VOI) of each sphere in Symbia SPECT studies.

The exponential curve fitting the RC values was performed using the Igor software [Igor Pro, version 4.01, Wavemetrics, Inc, 1988-2000, Oregon, USA]. RC data errors were evaluated by taking into account the Poisson distribution of the SPECT acquired counts and the errors in activity measurement, volume and time interval estimation.

Monte Carlo simulation for ^{99m}Tc and ^{177}Lu

Monte Carlo simulations of the experiments performed with ^{99m}Tc and ^{177}Lu have been performed via SIMIND v6.1.

The Monte Carlo simulation code SIMIND is a photon-tracking program developed by Professor Michael Ljungberg (Medical Radiation Physics, Department of Clinical Sciences, Lund, Lund University, Sweden). SIMIND describes a standard clinical SPECT camera and provides projected images from user defined attenuation map and activity distribution.

Both ^{99m}Tc and ^{177}Lu were studied via SIMIND: the main parameters set for the Monte Carlo simulations are listed in Table 6.

In order to obtain the three-dimensional studies, the projected images produced via SIMIND were reconstructed using CASToR (Customizable and Advanced Software for Tomographic Reconstruction [14]), an open-source toolkit for tomographic reconstruction for both emission and transmission exams. CASToR applies an iterative reconstruction technique, in particular an OSEM-3D with 10 iterations and 8 subsets was used including scatter and attenuation correction with a stationary PSF modelled as a 3D isotropic Gaussian.

Results

As preliminary step, we compared the profiles of a uniform filled cylinder with the radionuclides used in this study, ^{99m}Tc or ^{177}Lu , measured experimentally with the Monte Carlo calculated ones. Figure 2 (top) shows the result for ^{99m}Tc , while the figure 2 (bottom) shows the results for ^{177}Lu . The error bar associated with each position of the measured profile has been calculated as the square root of the counts associated with the position.

Planar Spatial Resolution and Sensitivity

Figure 3 (top) shows the comparison between the experimentally measured and Monte Carlo calculated spatial resolution plotted as function of the source-detector distance for ^{99m}Tc while the figure 3 (bottom) shows the comparison between the experimentally measured and Monte Carlo calculated sensitivity plotted as function of the source-detector distance for ^{99m}Tc . Experimental results are in good agreement with the results obtained from SIMIND simulation.

Figure 4 shows the data about the spatial resolution for the peaks 113 keV and 208 keV of ^{177}Lu as function of source detector distance, while the figure 5 shows the experimentally measured and Monte Carlo calculated sensitivity as function of source detector distance for the two peaks of ^{177}Lu . Even in this case, the experimental results are in good agreement with the simulated ones, apart from the 208 keV sensitivity: the experimental values are nearly 14% lower than those obtained with SIMIND. Ramonaheng *et al.* [9] have reported for 208 keV peak of ^{177}Lu the experimental and MC (SIMIND) simulated data of 10.0 ± 0.3 cps/MBq and 10.3 cps/MBq, respectively.

In table 7, the measured and the simulated sensitivity at a distance of source-detector of 10 cm both for ^{99m}Tc and ^{177}Lu are reported.

CF and RC for ^{99m}Tc and ^{177}Lu

Symbia Intevo CF has been evaluated for all the uniformity phantom acquisitions performed. Two cylindrical ROIs were used for CF evaluation: the type 1 ROI had a volume 30% larger than the volume of Jaszczak phantom but with the same geometrical center, while the type 2 ROI had a volume 30% smaller than the volume of Jaszczak phantom but with the same geometrical center. The errors associated with experimental results take into account:

- the Poisson distribution of the counts;
- errors in the evaluation of phantom volume;
- error in activity evaluation through the calibrator (standard deviation of the measurement of the syringe samples, but also the systematic error of the calibrator itself);
- the standard deviation of the VOIs volume values;
- error in time interval evaluation.

The ^{99m}Tc calculated CF value for the type 1 ROI was 110.1 ± 5.5 cps/MBq for experimental data while for SIMIND data the calculated value was 100.1 ± 0.3 cps/MBq. The CF value calculated by using the type 2 ROI were 111.8 ± 5.6 cps/MBq and 101.7 ± 0.3 cps/MBq respectively for experimental and simulated data.

In figure 6, the RC experimental values for ^{99m}Tc are compared with the RC values obtained by using Monte Carlo simulation and reconstructed by CASToR software. For partially compensating the CDR function, a 2D gaussian distribution has been used in the reconstruction process, and in figure 6 we reported the results for three standard deviations corresponding to the gamma camera spatial resolution at the minimum, maximum and central distance between Jaszczak SPECT phantom and collimator.

In order to obtain the CF factor for Lutetium, the previous procedure has been

repeated, except that the starting activity used to fill the phantom, 2818 ± 70 MBq was so high that gamma camera dead-time had effect on the calculated CF value. Hence, starting from dead-time response of modern gamma camera, typically described by the paralyzable model, it is possible to derive the measured calibration factor CF_m as function of the true calibration factor CF_t , the source activity A and the gamma camera apparent dead-time τ_a (the ratio between the true dead-time τ and the fraction of detected events occurring within the selected energy window w_f)[15]

$$CF_m = CF_t \cdot e^{-CF_t \cdot A \cdot \tau_a} \quad (1)$$

In figure 7 is shown the CF values obtained as function of phantom activity: a curve fitting procedure by using the eq. 1 allowed us to calculate the $CF_t = 18.3 \pm 1.0$ cps/MBq for type 1 ROI, while the $CF_t = 18.6 \pm 1.0$ cps/MBq for type 2 ROI. The estimated value for apparent dead-time $\tau_a = 2.3 \pm 1.6 \mu s$ is compatible with the result reported by Frezza et al. [16]. The results of CF for type 1 ROI are reported in Table 8.

The same uniformity phantom acquisitions have been repeated with SIMIND, in order to find CF for Lutetium; it is important to underline that CASToR can reconstruct studies taking into account only one peak at time. So, two different values for CF (one for the peak at 113 keV and one for the peak at 208 keV) have been obtained. Results are in Table 8. The "right peak" for dosimetry tasks is the second one, because of the less scattering/down scattering and the major abundance. RC factors have been evaluated from 1.4 ml to 1000 ml, using pockets filled with Lutetium. The final fit is shown in figure 8 weighted for the errors.

Discussion

The results obtained for the parameters acquired in planar imaging show an excellent agreement with the simulated data except for the sensitivity of the gamma camera for the 208 keV photons of ^{177}Lu , in this case the value calculated with the MC simulation is 10% higher than the experimentally measured value.

A critical element in the experimental evaluation of sensitivity is the accuracy with which the activity used in the experimental tests is measured. The certified activity of the ^{177}Lu sample provided by the ITM is known with an error of 10%, and this sample is used to determine the conversion factor k between the current measured by the dose calibrator and the activity of ^{177}Lu , assuming that the activity meter behaves in a linear manner over the entire measurement range of the activities we use. This assumption introduces at least 10% error in the calculation of experimental sensitivity.

The parameters acquired in tomographic mode, CF and RC, require a further step to be calculated: tomographic reconstruction using appropriate software. Usually, for SPECT tomographic reconstruction it is used an iterative reconstruction algorithm that allows to include in the projection operator the following three contributions: the response function of the collimator, the contribution of scatter and the contribution of tissue attenuation of radiation. Thus, the parameters calculated from the reconstructed images depend on how correct the estimate of the three

contributions is. For this reason, we checked the effects of these three contributions both in the calculation of the CF and the RC curve.

In the calculation of the CF using the simulated data with SIMIND we have noticed as it was critical the estimation of the contribution of the scatter, in particular for the ^{99m}Tc using the dual energy window (DEW) method and a weight factor w for the calculation of the scatter contribution in each projection. By changing the weight factor w starting from 0.5, theoretical weight of DEW method, to 0.87, value estimated by the ^{99m}Tc simulated energy spectrum with fitting procedure, we have obtained values between 107.3 ± 0.3 cps/Mbq and 93 ± 0.3 cps/Mbq. The value shown in Table 8 is the one obtained with the value of $w=0.667$ used by the Symbia Intevo software.

For the estimation of the RC curve using the simulated data with SIMIND we noticed that the correction for the collimator response function was critical. The software CASTOR at the moment allows to include a Gaussian collimator response function not dependent on the distance. For this reason, we have used Gaussian distributions with FWHM values ranging from the minimum value to the maximum value which depends on the distance of the activity from the collimator. For ^{99m}Tc the minimum FWHM is 9.18 mm and the maximum FWHM 13.5 mm values obtained from the figure 2 and taking into account the minimum and maximum distance of the activity present in the cylindrical phantom from the collimator. The same was done for ^{177}Lu . So, in figure 6 we reported the values of the RC curve for ^{99m}Tc corresponding to three different FWHM values and as you can see the curve RC that matches better with the experimental data is the one obtained with the Gaussian distribution with FWHM corresponding to the distance of the center of the cylindrical phantom from the collimator. In figure 8 we reported the RC curve for ^{177}Lu .

Conclusions

In this study the best parameters for reconstruction and correction of SPECT-CT analysis have been found, in order to standardize successive study and at the same guaranteeing the best achievable image quality and a correct activity evaluation. Moreover, it has been proven that SIMIND is a useful tool to simulate gamma cameras, using several radionuclides for different purpose both in diagnostic and therapeutic fields. In particular, in the nuclear medical therapeutic field, the role of targeted therapies is emerging for the treatment of neuroendocrine tumors, prostate cancer and other solid neoplasms. These treatment modalities, which can also be defined as endoradiotherapy, aim to concentrate ionizing radiation on the lesions and, at the same time, limit as much as possible the irradiation of healthy tissues and potential organs at risk (kidney, bone marrow, glands salivary ...). A predictive or peri-therapeutic dosimetry evaluation is therefore mandatory to optimize therapeutic efficacy and reduce the risk of toxicity, especially in those therapeutic models that have not yet achieved complete standardization. At the same time, the EURATOM 59 directive (implemented in the Italian state by legislative decree 101) indicates the need to carry out a dosimetric evaluation in all therapeutic practices including the use of ionizing radiation. Hence the need to develop friendly dosimetric models based on increasingly precise and accurate calculation algorithms.

Declarations

Ethics approval and consent to participate

Not applicable

Consent for publication

Not applicable

Availability of data and materials

Not applicable

Competing interests

The authors declare that they have no competing interests.

Funding

This research has been partially supported by the Regione Emilia Romagna grant funded on "Programma operativo Fondo sociale europeo 2014/2020".

Authors' contributions

SDB was responsible for the tomographic acquisitions, tomographic image data analysis and she wrote the first draft of manuscript. LL was responsible for the planar acquisitions and planar image data analysis. GDD was responsible for the MC simulations, the MC data reconstruction, the MC data analysis and he wrote the manuscript. AT, ET, MCL were involved in the experimental design of this study, LU was involved in the chemistry management of Lu-177, MB supervised the project. All authors were involved in reviewing the manuscript, and they all read and approved the final manuscript.

Acknowledgements

Not applicable

Author details

¹Department of Physics and Earth Science, University of Ferrara, via Saragat 1, 44122 Ferrara, IT. ²Medical Physics Unit, University Hospital, 44124 Ferrara, IT. ³San Bortolo Hospital, 44124 Vicenza, IT. ⁴Nuclear Medicine Unit, University Hospital, 44124 Ferrara, IT. ⁵Department of Translational Medicine, University of Ferrara, via Fossato di Mortara, 70 c/o viale Eliporto, 44124 Ferrara, IT.

References

1. Zaidi H. Relevance of accurate Monte Carlo modeling in nuclear medical imaging. *Med Phys.* 1999;26:574–608.
2. Liu S, Famcombe TH. Collimator-detector response compensation in quantitative SPECT reconstruction. In: 2007 IEEE Nuclear Science Symposium Conference Record: 27 October - 3 November 2007; Hawaii. IEEE Nuclear Science; 2007. p. M19–327.
3. Chun SY, Fessler JA, Dewaraja YK. Correction for Collimator-Detector Response in SPECT Using Point Spread Function Template. *IEEE Trans Med Imaging.* 2013;32:295–305.
4. Willowson K, Bailey DL, Baldock C. Quantitative SPECT reconstruction using CT-derived corrections. *Phys Med Biol.* 2008;53:3099–3112.
5. Pacilio M, Cassano B, Pellegrini R, Di Castro E, Zorzi A, De Vincentis G, et al. Gamma camera calibrations for the Italian multicentre study for lesion dosimetry in 223Ra therapy of bone metastases. *Phys Medica.* 2017;41:117–23.
6. Zeintl J, Vija AH, Yahil A, Hornegger J, Kuwert T. Quantitative accuracy of clinical 99mTc SPECT/CT using ordered-subset expectation maximization with 3-dimensional resolution recovery, attenuation, and scatter correction. *J Nucl Med.* 2010;51:921–8.
7. Dong X, Saripan MI, Mahmud R, Mashohor S, Wang A. Characterization of SIEMENS Symbia T SPECT camera in Monte Carlo simulation environment. *Pakistan Journal of Nuclear Medicine.* 2019;8(1):18–26.
8. Toossi MTB, Islamian PJ, Momenzhad M, Ljungberg M, Naseri SH. SIMIND Monte Carlo simulation of a single photon emission CT. *Journal of Medical Physics.* 2010;35(1):42–47.
9. Ramonaheng K, van Staden JA, du Raan H. Validation of a Monte Carlo modelled gamma camera for Lutetium-177 imaging. *Appl Radiat Isot.* 2020;163:109200.
10. Ejeh JE, van Staden JA, du Raan H. Validation of SIMIND Monte Carlo Simulation Software for Modelling a Siemens Symbia T SPECT Scintillation Camera. In: *World Congress on Medical Physics and Biomedical Engineering 2018. IFMBE Proceedings*, vol 68/1. Springer, Singapore. IUPESM; 2018. p. 573–576.
11. Morphis M, van Staden JA, du Raan H, Ljungberg M. Validation of a SIMIND Monte Carlo modelled gamma camera for Iodine-123 and Iodine-131 imaging. *Heliyon.* 2021;7(6):e07196.
12. Ljungberg M. The SIMIND Monte Carlo program. In: M Ljungberg MAK S E Strand, editor. *Monte Carlo calculations in nuclear medicine: Applications in diagnostic imaging*. 2nd ed. Boca Raton: CRC Press; 2012. p. 111–128.
13. Ljungberg M, Celler A, Konijnenberg MW, Eckerman KF, Dewaraja YK, Sjögren-Gleisner K. MIRD Pamphlet No. 26: Joint EANM/MIRD Guidelines for Quantitative 177Lu SPECT Applied for Dosimetry of Radiopharmaceutical Therapy. *J Nucl Med.* 2016;57:151–162.
14. Merlin T, Stute S, Benoit D, Bert J, Carlier T, Comtat C, et al. CASToR: a generic data organization and processing code framework for multi-modal and multi-dimensional tomographic reconstruction. *Phys Med Bio.* 2018;63:151–162.
15. S R Cherry MEP J A Sorenson. *Physics in Nuclear Medicine*. Philadelphia: Elsevier Saunders; 2012.
16. Frezza A, Desport C, Uribe C, Zhao W, Celler A, Després P, et al. Comprehensive SPECT/CT system characterization and calibration for 177Lu quantitative SPECT (QSPECT) with dead-time correction. *Eur J Nucl Med Mol Imaging.* 2020;7(10):1–22.

- 1
2
3
4
5
6
7
8
9
17. Bé MM, Duchemin B, Lamé J, Morillon C, Piton F, Browne E, et al. Table de Radionucléides. vol. 1. DAMRI/LPRI BP 52, F-91193 Gif-sur-Yvette Cedex, France: Commissariat à l'Énergie Atomique; 1999.
 18. Uccelli L, Boschi A, Cittanti C, Martini P, Panareo S, Tonini E, et al. 90Y/177Lu-DOTATOC: From Preclinical Studies to Application in Humans. *Pharmaceutics*. 2021;13:1463.

10 Figures

11
12
13
14

Figure 1 Experimental Setup Example of experimental configuration: on the left, the uniform phantom is shown; on the right, the acquisition moment for Tc-99m.

15
16
17
18
19
20
21

Figure 2 Comparison of experimental and simulated projection profiles. (top) Plot of experimentally measured and Monte Carlo simulated profile of uniform cylinder filled with ^{99m}Tc . (bottom) Plot of experimentally measured and Monte Carlo simulated profile of uniform cylinder filled with ^{177}Lu .

22
23
24
25
26
27

Figure 3 Spatial resolution and sensitivity for ^{99m}Tc . (top) Plot of spatial resolution as function of distance between source and detector for ^{99m}Tc . (bottom) Plot of sensitivity as function of distance between source and detector for ^{99m}Tc .

28
29
30
31
32

Figure 4 Spatial resolution for ^{177}Lu . Plot of spatial resolution as function of distance between source and detector for ^{177}Lu : 113 keV peak (top), 208 keV peak (bottom).

33
34
35
36
37

Figure 5 Sensitivity for ^{177}Lu . Plot of sensitivity as function of distance between source and detector for ^{177}Lu : 113 keV peak (top), 208 keV peak (bottom).

38
39
40
41
42

Figure 6 RC for ^{99m}Tc . Plot of measured and calculated by MC data recovery coefficients (RC) for ^{99m}Tc as function of sphere volumes.

43
44
45
46
47

Figure 7 CF for ^{177}Lu . Plot of calibration factor coefficients (CF) for ^{177}Lu as function of activity in the phantom.

48
49
50
51
52

Figure 8 RC for ^{177}Lu . Plot of measured and calculated by MC data recovery coefficients (RC) for ^{177}Lu as function of sphere volumes.

53 Tables

54
55
56
57
58
59
60
61
62
63
64
65

Table 1 Decay characteristics of both Tc-99m and Lu-177; data from [17, 18]

Isotope	Half-life	Strongest γ emission E_{γ} [keV] (I_{γ} [%])	Max β energy E_{max} [keV]
Tc-99m	6.01 h	140.5 (88.5)	436.2
Lu-177	6.65 d	112.9 (6.2) 208.4 (10.4)	498.3

Table 2 Main Symbia parameters, taken from Symbia Intevo data sheet

Crystal size	59.1 × 44.5 cm
Crystal thickness	9.5 mm
PMT total number	59
PMT array	Hexagonal
System resolution at 10 cm, 140 keV	7.5 mm
Energy resolution at 140 keV	9.9%
Sensitivity at 10 cm, 140 keV	91 cps/MBq
SPECT reconstruction matrix size	128x128

Table 3 The lower and upper scatter windows for technetium and lutetium main peaks are listed.

Radionuclide	Main peak [keV]	PW range [keV]	LSW range [keV]	USW range [keV]
Tc-99m	140.5	123.9-151.4	103.2 - 123.9	not used
Lu-177	113	102.7-119.4	86.1-102.7	119.4 - 128.2
Lu-177	208	189.3-220.0	168.8-189.3	not used

Table 4 The six spheres of the Jaszczack phantom with their respective activity and the background are shown. Each of the value reported in this Table is the mean value of five different measurements, with a standard deviation less than 1%. These errors must be added to the 10% error on the Activity (certified by the producer).

Sphere Volume [ml]	Sphere Diameter [mm]	Activity [MBq]
0.5	9.8	4.8
1.0	12.4	4.4
2.0	15.6	4.5
4.0	18.9	4.7
8.0	24.8	4.7
16.0	31.2	4.6
Phantom Volume [ml]		Activity [MBq]
6800		131.7

Table 5 The five spheres of the NEMA PET phantom with their respective activity and background are shown. Each of the value reported in this Table is the mean value of five different measurements, with an associated error of less than 11%.

Sphere Volume [ml]	Sphere Diameter [mm]	Activity [MBq]
1.4	13.0	8.3
2.5	17.0	8.4
5.0	22.0	8.6
11.0	28.0	8.7
26.0	37.0	7.5
Phantom Volume [ml]		Activity [MBq]
9600		201.0

Table 6 Main parameters inserted in SIMIND's CHANGE program for horizontal cylinder Tc-99m filled.

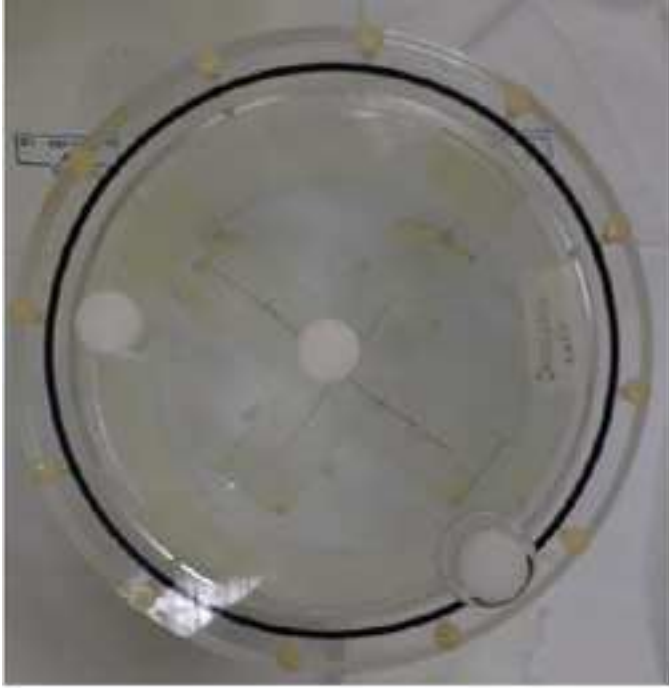
	Tc-99m	Lu-177
Photon energy	140 keV	113 keV and 208 keV
Source type	Horizontal cylinder	Horizontal cylinder
Energy resolution	9.9% @140.5keV	9.9% @140.5keV
Intrinsic Resolution	0.38 mm	0.38 mm
Photons per projection	10^7	10^7
Distance to detector (circular orbit)	25 cm	25 cm
Matrix Size	128x128	128x128
Acceptance angle	45°	45°
Rotation mode	CW	CW
Rotation angle step	5.625°	5.625°
Number of projection	64	64
Collimator	Sy-LEHR	Sy-ME

Table 7 Comparison of measured planar System Sensitivity with Monte Carlo results. All parameters have been measured at distance of 10 cm from collimator.

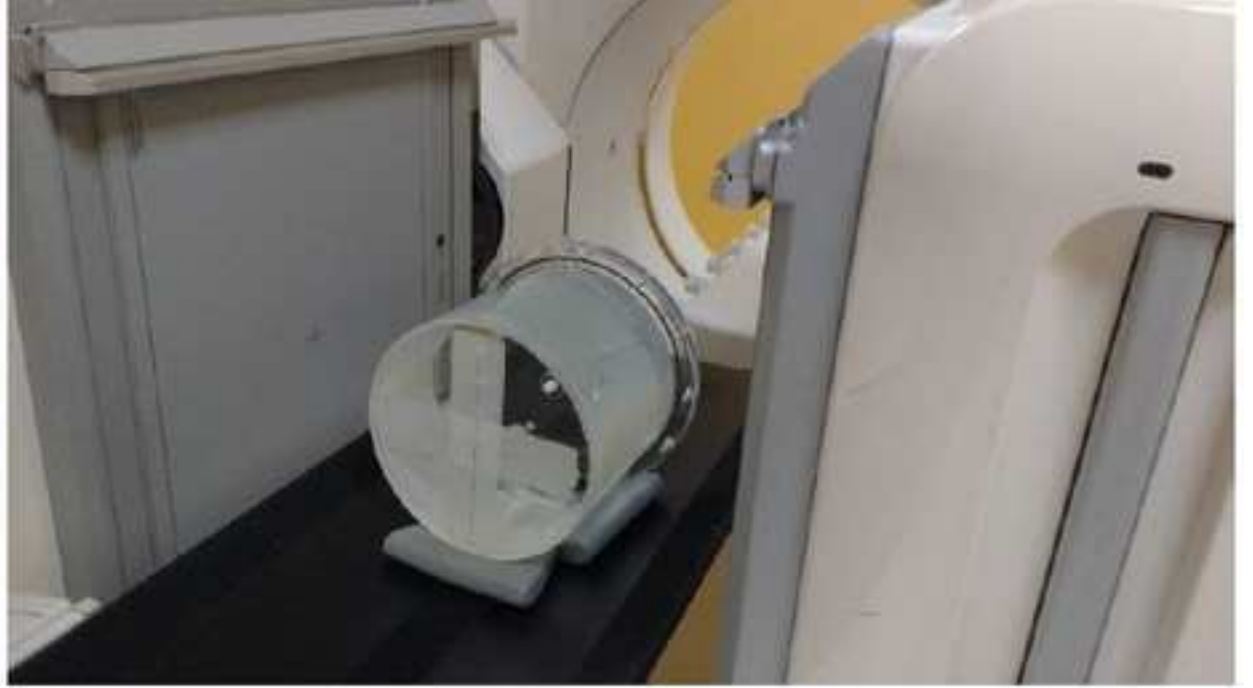
Parameter	Radioisotope	Main peak [keV]	Experimental	Simulated
Sensitivity [cps/MBq]	Tc-99m	140.5	88.0 ± 4.4	89.4 ± 0.5
Sensitivity [cps/MBq]	Lu-177	113.0	9.9 ± 0.5	9.7 ± 0.1
Sensitivity [cps/MBq]	Lu-177	208.0	9.6 ± 0.5	10.9 ± 0.2

Table 8 CF evaluation study for Tc-99m with Isocontour and Ellipsoid contouring with Symbia NET workflow. CF evaluation study for Tc99m with Isocontour and Ellipsoid contouring with Monte Carlo Code SIMIND.

Parameter	Method	Radioisotope	Main peak [keV]	Experimental	Simulated
CF [cps/MBq]	Ellipsoid	Tc-99m	140.5	110.1 ± 5.5	100.1 ± 0.3
CF [cps/MBq]	Ellipsoid	Lu-177	113.0+208.0	18.3 ± 1.0	20.4 ± 0.7



Left



Right

